International Journal For Technological Research In Engineering
Volume 2, Issue 6, February-2015 *ISSN (Online): 2347 - 4718*

A NOVEL DC-DC CONVERTER FOR AN AUTONOMOUS PHOTO VOLTAIC WATER PUMPING SYSTEM

C. Asenshiya[1], M. Premalatha[2]
[1]Assistant Professor, [2]PG Scholar
Department of EEE, Thangavelu Engineering College, Chennai-600097

Abstract: This paper proposes a new converter for photovoltaic (PV) water pumping or treatment systems without the use of chemical storage elements, such as batteries. The converter is designed to drive a three-phase induction motor directly from PV energy. The use of a three-phase induction motor presents a better solution to the commercial dc motor water pumping system. The development is oriented to achieve a more efficient, reliable, maintenance-free, and cheaper solution than the standard ones that use dc motors or low-voltage synchronous motors. The de- veloped system is based on a current-fed multiresonant converter also known as resonant two-inductor boost converter (TIBC) and a full-bridge three-phase voltage source inverter (VSI). The classic topology of the TIBC has features like high voltage gain and low input current ripple. In this paper, it is further improved with the use of a nonisolated recovery snubber along with a hysteresis controller and the use of a constant duty cycle control to improve its efficiency. Experimental results show a peak efficiency of 91% at a rated power of 210 W for the dc/dc converter plus the three-phase VSI and a peak efficiency of 93.64% just for the dc/dc converter. The system is expected to have a high lifetime due to the inexistence of electrolytic capacitors, and the total cost of the converter is below 0.43 U$/Wp. As a result, the system is a promising solution to be used in isolated locations and to deliver water to poor communities.
Index Terms: AC motor drives, dc–ac power conversion, dc–dc power conversion, photovoltaic (PV) power systems, solar power generation.

I. INTRODUCTION

Currently over 900 million people in various countries do not have drinkable water available for consumption. Of this total, a large amount is isolated, located on rural areas where the only water supply comes from the rain or distant rivers. This is also a very common situation in the north part of Brazil, where this work was developed. The unavailability of electric power rules out the pumping and water treatment through conventional systems. One of the most efficient and promising way to solve this problem is the use of systems supplied by photovoltaic (PV) solar energy. This kind of energy source is becoming cheaper and has already been put to work for several years without the need of maintenance. Such systems are not new and are already used for more than three decades. Nevertheless, until recently, the majority of the available commercial converters in Brazil are based on an intermediate storage system, performed with the use of lead-acid batteries, and dc motors to drive the water pump. More sophisticated systems have already been developed with the use of a low-voltage synchronous motor, but these, although presenting higher efficiency, are too expensive to be used in poor communities that need these systems. The batteries allow the motor and pump system to always operate at its rated power even in temporary conditions of low solar radiation. This facilitates the coupling of the electric dynamics of the solar panel and the motor used for pumping. Generally, the batteries used in this type of system have a low life span, only two years on average, which is extremely low compared to the useful life of 20 years of a PV module. Also, they make the cost of installation and maintenance of such systems substantially high. Furthermore, the lack of battery replacement is responsible for the failure of such systems in isolated areas. The majority of commercial systems use low-voltage dc motors, thus avoiding a boost stage between the PV module and the motor. Unfortunately, dc motors have lower efficiency and higher maintenance cost compared to induction motors and are not suitable for applications in isolated areas, where there is no specialized personnel for operating and maintaining these motors. Another problem is that low-voltage dc motors are not ordinary items in the local markets. Because of the aforementioned problems, this work adopted the use of a three phase induction motor, due to its greater robustness, lower cost, higher efficiency, availability in local markets, and lower maintenance cost compared to other types of motors. The design of a motor drive system powered directly from a PV source demands creative solutions to face the challenge of operating under variable power restrictions and still maximize the energy produced by the module and the amount of water pumped. These requirements demand the use of a converter with the following features: high efficiency due to the low energy available; low cost to enable its deployment where it is most needed; autonomous operation no specific training needed to operate the system; robustness minimum amount of maintenance possible; and high life span comparable to the usable life of 20 years of a PV panel. This paper proposes a new dc/dc converter and control suit- able for PV water pumping and treatment that fulfill most of the aforementioned features.The output voltage is four times of the conventional full-bridge voltage rectifier, which helps to reduce the turns of the secondary winding and decrease the parasitic parameters of the transformer. An advanced symmetrical voltage quadrupler rectifier (SVQR) is used for the high output voltage and high step-up dc-dc conversion applications. The output capacitor voltage balance can be realized naturally, which makes the voltage quadrupler more suitable for the 760 V dc-bus-based grid-connected PV generation systems due to the relatively low voltage of the aluminum electrolytic capacitors. Output voltage of SVQR Vout is four times of Vs , which benefits to reduce the number of turns greatly on the secondary side compared with the voltage doubler circuits.

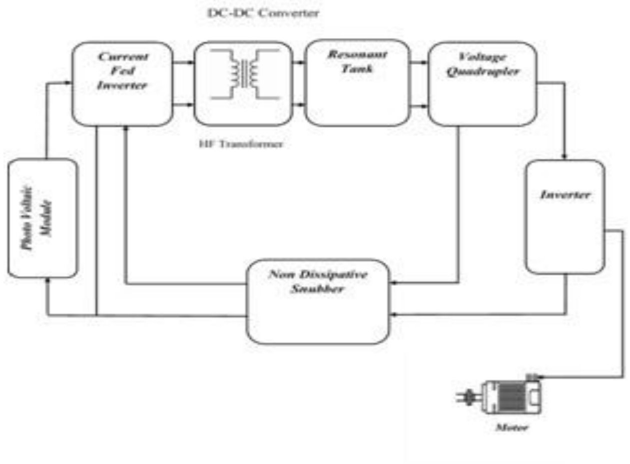

Fig. 1.Simplified block diagram of the proposed system.

II. PROPOSED CONVERTER

To ensure low cost and accessibility of the proposed system, it was designed to use a single PV module. The system should be able to drive low-power water pumps, in the range of 1/3 hp, more than enough to supply water for a family. Fig. 1 presents an overview of the proposed system. The energy produced by the panel is fed to the motor through a converter with two power stages: a dc/dc two-inductor boost converter (TIBC) stage to boost the voltage of the panels and a dc/ac three-phase inverter to convert the dc voltage to three-phase ac voltage. The inverter is based on a classic topology (three legs, with two switches per leg) and uses a sinusoidal pulse width modulation (PWM) (SPWM) strategy with 1/6 optimal third harmonic voltage injection as proposed in [9]. The use of this PWM strategy is to improve the output voltage level as compared to sinusoidal PWM modulation. This is a usual topology, and further analyses on this topology are not necessary. For the prototype used to verify the proposed system, a careful selection of the voltage source inverter (VSI) components is more than enough to guarantee the efficiency and cost requirements. The required dc/dc converter for this kind of system needs to have a large voltage conversion ratio because of the low-voltage characteristic of the PV panels and small input current ripple so that it does not cause oscillation over the maximum power point (MPP) of the PV module [10]–[12], thus ensuring the maximum utilization of the available energy. The commonly used isolated voltage-fed converters normally have a high input current ripple, which forces the converter to have large input filter capacitors. These are normally elec- trolytic, which are known to have a very small lifetime and thus affect the overall life span and mean time before failure of the converter. Furthermore, the inherent step-down char- acteristic of the voltage-fed converters, the large transformer turns ratio needed to boost the output voltage, the high output diode voltage stress, and the need of an LC output filter [13] make voltage-fed converters not the best choice for this application. Current-fed converters are normally derived from the boost converter, having an inherent high step-up voltage ratio, which helps to reduce the needed transformer turns ratio. Although the current-fed topologies have all the aforementioned advantages, they still have problems with high voltage spikes created due to the leakage inductance of the transformers and with high voltage stress on the rectifying diodes. One of the solutions to the current-fed PWM converters is the use of resonant topologies able to utilize the component parasitic characteristics, such as the leakage inductance and winding capacitance of transformers, in a productive way to achieve zero current switching (ZCS) or zero voltage switch- ing (ZVS) condition to the active switches and rectifying diodes.

In this paper, the use of a modified TIBC for the first-stage dc/dc converter is proposed, due to its very small number of components, simplicity, high efficiency, easy transformer flux balance, and common ground gate driving for both switches. In addition, the input current is distributed through the two boost inductors having its current ripple amplitude halved at twice the PWM frequency. This last feature minimizes the oscillations at the PV module operation point and makes it easier to achieve the MPP.

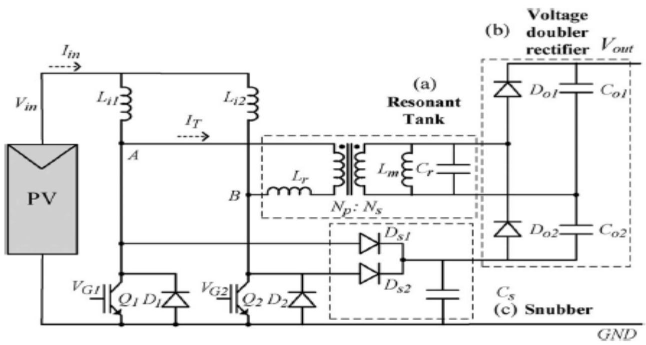

Fig. 2.Modified TIBC topology: (a) resonant tank, (b) voltage doublerrectifier, and (c) snubber.

In its classical implementation, the TIBC is a hard-switchedoverlapped pulse-modulated converter; this way, at least one ofthe switches is always closed, creating a conduction path for theinput inductor current. Nevertheless, the TIBC can be modifiedto a multiresonant converter by adding a capacitor at the transformer’s secondary winding. A multiresonant tankis formed by the magnetizing inductance of the transformer,its leakage inductance, and the added capacitor Fig. 2(a). The intrinsic winding capacitance of the transformeris included in the resonant capacitor. By adding this capacitor and using the parasitic componentsof the transformer to create the resonant tank, it is possibleto achieve ZCS condition for the input switches and outputrectifying diodes, and this enables the converter to operate athigh frequencies with greater efficiency.With the use of a voltage doubler rectifier at the secondaryside of the transformer, as shown in Fig. 2(b), it is possible toreduce the transformer turns ratio, the necessary ferrite core,and the voltage stress on the MOSFETs to half of the originalones. As a result, the transformer is cheaper, the MOSFETsare cheaper, and the number of diodes in the secondary side ishalved. Also, the output dc bus capacitor can be integrated withthe capacitors of the rectifier, particularly because the secondstagethree-phase VSI has almost dc input current, exemptingthe bus capacitor from any ac decoupling current. A modification in the control strategy of the proposed converteris also proposed, when compared to the classical TIBCcontrol. Section IV shows that, for the application of a PV water pumping system, the correct design of converter voltage gainmakes the converter able to operate with a constant gain, usinga fixed duty cycle modulation for the primary switches. To solvethe minimum load condition, the use of a hysteresis controllerfor the dc output voltage of the first stage is proposed. Whenoperating below the minimum required load, an uncontrolledincrease of output voltage will be seen, and once this voltagereaches the upper threshold, both primary switches are turnedoff. This would be impossible in all the previously reported implementationsof the TIBC. However, with the added snubber,even with both switches turned off, there is still a path for theinput inductors' current. Their energy is directly transferred tothe snubber capacitor Cs. This capacitor must be sized to havea minimum voltage increase during this hysteresis action. Asthis capacitor is in series with the output rectifier, the samevoltage increase will be noted in the output voltage. Afterthe switches are turned off and the input inductors' energyis transferred to the snubber, the output voltage will start todecrease, reaching the lower hysteresis threshold and restartingthe PWM operation with the fixed duty cycle.

III. OPERATION PRINCIPLE

In the hard-switched operation of the TIBC, the two primaryswitches $Q1$ and $Q2$ operate at an overlapped duty cycle switchingscheme to guarantee a conduction path for the primaryinductor current. When both $Q1$ and $Q2$ are turned on, $Li1$ and$Li2$ are charged by the input energy. When $Q1$($Q2$) is opened,the energy stored in $Li1$($Li2$) is transferred to $Co1$($Co2$)through the transformer and the rectifier diode $Do1$($Do2$).Once the multiresonant tank is introduced, two differentresonant processes occur: 1)When both switches are closed, theleakage inductance Lrparticipates along with capacitance Crin the resonance at the primary current switching and currentpolarity inversion, allowing ZCS operation for the primaryswitches, and 2) during the conduction time interval (between$t4$ and $t5$ in Fig. 3), when at least one of the switches is open,$Lr$is associated in series with $Li1$ or $Li2$, not participating onthe transformer's secondary current resonance, formed only byLm and Cr. The key waveforms for a switching period of theTIBC are presented in Fig. 3. In this figure, $VgQ1$ and $VgQ2$are the gate signals of the switches $Q1$ and $Q2$, respectively;$VdsQ2$ is the drain-to-source voltage of MOSFET $Q1$; $IQ2$ isthe current of MOSFET $Q2$; VT is the voltage at the primaryof the transformer; IT is the current at the primary of thetransformer; $ILi1$ and $ILi2$ are the currents of inductors $Li1$ and$Li2$, respectively; and Iin is the input current of the converterand also the current supplied by the PV panel.At time $t1$, the rectifying diode $Do1$ is already conducting,and the voltage on resonant capacitor Cr is clamped at+Vout/2. At this instant, the switch $Q1$ is activated by $VgQ1$. As the switch is turned on, its voltage drops to zero, and the snubber diode $Ds1$ is forced to stop conducting. From $t1$ to $t2$, Cr transfers its energy to the leakage inductance Lr, beginning the primary switch's resonant process and forcing the current $IQ2$ on the switch $Q2$ to decrease. At the time $t2$, the rectifying diode$Do1$ stops conducting, and Cr continues to resonate with the magnetizing inductance Lm. From $t2$ to $t3$, the primary switch's resonance ($Q2$) continues to force its current to decrease until it reverses its polarity. When $IQ2$ is negative; the switch can be turned off. This happens at instant $t3$ when $VgQ2$ is forced to zero At the time $t3$, the voltage $VdsQ2$ starts to increase, $Q2$ is completely blocked, and the snubber diode $Ds2$ begins to conduct, transferring energy directly to the snubber capacitor Cs. Between $t3$ and $t4$, Cr and Lm continue to resonate, decreasing the voltage on the doubler rectifier's input and on VCr. At instant $t4$, the voltage across Cr reaches $-V$out/2, and the rectifying diode $Do2$ starts to conduct, clamping VCrin $-V$out/2. From $t4$ to $t5$, the capacitor $Co1$ is charged, and the current of $Do2$ starts to decrease. At the instant $t5$, $Q2$ is turned on, initiating the resonant process on $Q1$. As $Q2$ is activated, $Ds2$ is forced to stop conduction. At the instant $t6$, the current in $Do2$ reaches zero, and $Do2$ stops conducting, reinitiating the resonance between Cr and Lm. From this moment, until the end of the switching period, the process repeats symmetrically as explained for the other input switch.

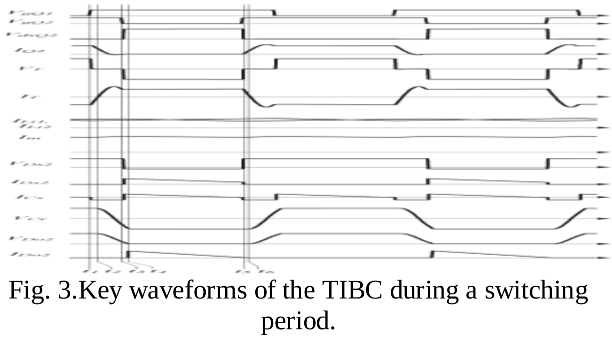

Fig. 3.Key waveforms of the TIBC during a switching period.

An extended description of multiresonant TIBC without thesnubber is presented and analyzed, resulting in a detailedmathematical modeling for both resonant processes during itsoperation. However, the analysis is based on severalcomplex mathematical models, and consequently, the presenteddesign method shows several dependent variables, which translatesin a design methodology difficult to be implemented. In this paper, a simplified methodology based on the effectof each resonant process, the resonant frequencies, andthe switching frequency is applied. Spice simulations and aprototype are used to show that, despite the simplicity of thedesign methodology, the correct operation of the converteris guaranteed, particularly the soft switching of the primaryswitches for the whole operating load range.Although the resonant process affects the output voltage,depending on the resonant tank component values and the load,this can be neglected because of its small influence and complexeffect.

IV. CONTROL OF THE SYSTEM

There are three main aspects in the proposed converter'scontrol: 1) During normal operation, a fixed duty cycle is usedto control the TIBC MOSFETs, thus generating an unregulatedhigh bus voltage for the inverter; 2) an MPP tracking (MPPT)algorithm is used along with a PI controller to set the speed ofthe motor and achieve the energy balance of the system at theMPP of the PV module; and 3) a hysteresis controller is usedduring the no-load conditions and start-up of the system. Eachof these aspects is described in the following sections.

A. Fixed Duty Cycle Control

One of the most important control aspects of this systemis the fact that it is possible to use an unregulated dc outputvoltage and a fixed duty cycle for the first-stage dc/dc converter.As a resonant converter, there are definite time intervals in theswitching period for the resonance process to occur. By alteringthe duty cycle or the switching period to control the outputvoltage, the converter may no longer operate at ZCS condition.Therefore, the fixed duty cycle is used to overcome these designproblems and ensure that the converter is going to operate inZCS condition despite the input voltage or output load.The duty cycle was chosen to guarantee that the amount oftransferred energy occurs during most part of the switchinginterval. Therefore, it is possible to transfer the same amount ofenergy with a smaller rms current. Therefore, the losses in theinput inductors (Li1 and Li2), in the MOSFETs (Q1 and Q2),and in the transformer are smaller. As a result, the efficiency ofthe converter improves.The operation with a fixed duty cycle makes the converterwork with a constant voltage gain Kv, almost independent ofthe input voltage. With the correct design of Kv, the systemwill always be able to transfer energy from the PV module tothe motor. Assuming that the converter is always operating atthe MPP of the solar panel, the output dc/dc converter voltage(dc bus voltage) will be with VMPP being the MPP voltage of the solar panel.

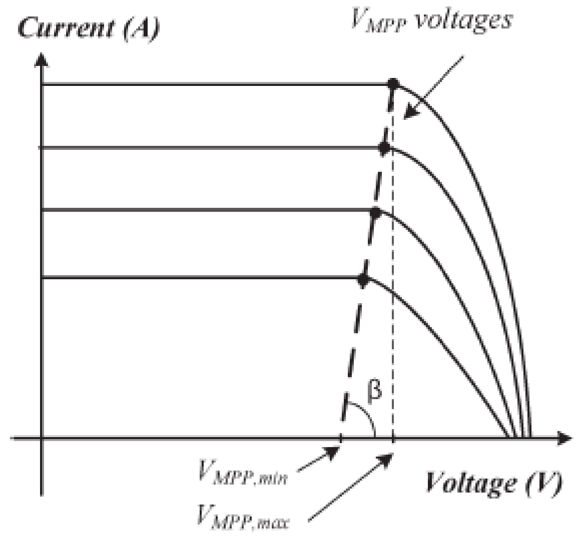

Fig. 4shows the *I–V* characteristic curves for a typical solar panel.

It is shown that the voltage at the MPP (*V*MPP) has only smallvariations for different radiation levels. The different *V*MPPpoints for various radiation levels are represented by the blackdashed line. Considering that nominal voltage is necessary to achievenominal power, Fig. 5 shows a comparison between the outputvoltage of the dc/dc converter (dashed line) and the minimumdc bus voltage required to operate the motor (solid line—cubicfunction) in the full power range. This minimum dc bus voltage was calculated by considering that the inverter is operating atthe maximum voltage with a modulation index of 1 (no over modulationis allowed). The correct design of Kvguaranteesthat the output voltage of the first stage will always be greaterthan the minimum voltage necessary to drive the motor.

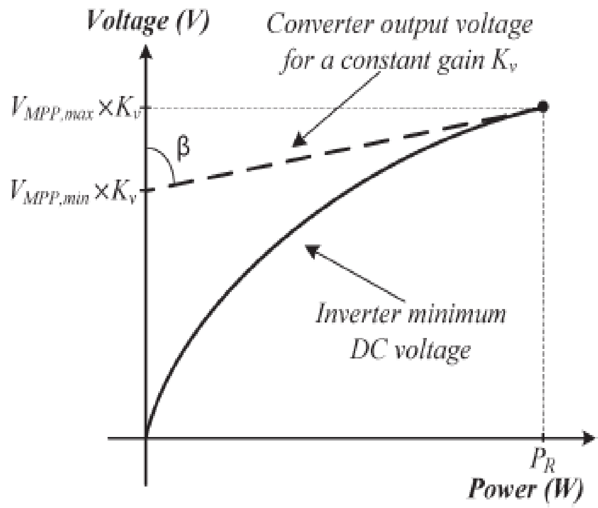

Fig. 5. DC bus value and minimum voltage needed for pump operation inconstant volt/hertz.

B. MPPT Control
The MPPT is a strategy used to ensure that the operatingpoint of the system is kept at the MPP of the PV panel. The widely used hill-climbing algorithm was applied due to itssimple implementation and fast dynamic response.This MPPT technique is based on the shape of the powercurve of the PV panel. This curve can be divided into twosides, to the left and to the right of the MPP. By analyzing thepower and voltage variation, one can deduce in which side ofthe curve the PV panel is currently operating and adjust thevoltage reference to get closer to the desired point. The voltagereference is used on a PI controller to increase or reduce themotor speed and consequently adjust the bus and panel voltageby changing its operating point.

C. Hysteresis Control
The main drawback of the classical TIBC is its inability tooperate with no load or even in low-load conditions. The TIBCinput inductors are charged even if there is no output current,and the energy of the inductor is lately transferred to the outputcapacitor raising its voltage indefinitely until its breakdown.Classically, the input MOSFET cannot be turned off becausethere is no alternative path for the inductor current. However,with the addition of the proposed snubber, the TIBC switchescan be turned off. Thus, a hysteresis controller can be set upbased on the dc bus voltage level. Every time a maximumvoltage limit is reached, indicating a low-load condition, thismode of operation begins. In this case, the switches are turnedoff until the dc bus voltage returns to a normal predefined level.As a result, the switching losses are reduced during this periodof time.

TABLE I
PANEL AND MOTOR PARAMETERS

Parameters	Values
PV Model	KD210GX
PV Power	210 W
PV Open circuit voltage (V_{OC})	29.9 V
PV Short circuit current (I_{SC})	6.98 A
PV Maximum MPP voltage ($V_{MPP,max}$)	26.6 V
Motor nominal power	0.2 HP
Motor nominal voltage (V_{rms})	220 V 3 ϕ
Motor nominal frequêncy	60 Hz

TABLE II
CONVERTER DESIGN SPECIFICATIONS

Parameters	Values
Converter Input Current Ripple	5 %
Nominal Bus Voltage	350 V
TIBC Switching Frequency	100 kHz
Inverter Switching Frequency	7.7 kHz
Constant voltage gain K	11.69
Transformer turns ratio N_s/N_p	2.25

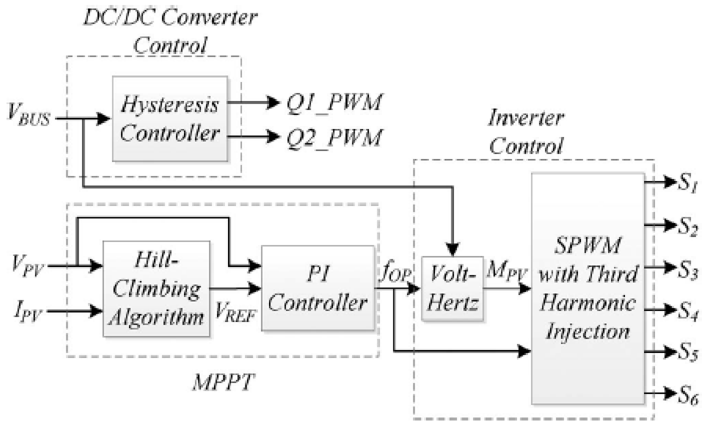

Fig. 6. Block diagram of the control system.

V. SIMULATION AND EXPERIMENTAL RESULTS
Fig. 7 shows the schematics used for the first-stageTIBC. All parasitic series resistances were included in the transformerand capacitors. The control of the primary MOSFETswas simulated using a fixed pulse modulation and a voltagecontrolledsource to implement the hysteresis control within thelimits of 380 V • } 10 V.

Fig. 8 shows the overlapped pulses used to control Q1 andQ2, the current in both input inductors, and the current in thePV module. It is observed that each one of the inductors has acurrent ripple at the converter switching frequency and out ofphase with each other; however, both currents are supplied bythe PV module, and when they are analyzed together (IPV), areduction in the ripple amplitude to half of the original onesis seen.

Fig. 9 shows the gate-to-source voltage, the drain-to-sourcevoltage, and current for one of the primary MOSFETs. It isobserved that there are no voltage spikes or increased voltagestress over the switches. In addition, the figure shows that bothturn-on and turnoff occurs at almost ZCS.

Fig. 10 shows voltage and current on the output rectifyingdiode Do1.It is shown that not only the primary MOSFETs areoperated under ZCS condition but also the rectifying diodes.The operation under ZCS condition allows the use of fastrecovery diodes instead of the expensive silicon carbide ones,thus reducing the total cost of the system.

Fig. 12 demonstrates a real time I–Vcurve, and the operating point of the system is emphasized bythe darker spot. The system starts its operation at the opencircuit voltage (VOC) and then stabilizes on the MPP. As thesolar radiation varies, the MPPs move. The system was able tostably track these points. The black dashed line shows all thepoints during a day.

Fig. 13(a) shows the current and voltage waveforms in one ofthe MOSFETs during a switching interval, with the converteroperating at full load. It is observed that ZVS is achieved forboth turn-on and turnoff events. Fig. 14(b) shows the TIBCoutput voltage (green line), the MOSFET Q1 drain-to-sourcevoltage (pink line), and the MOSFET Q1 current (orange line)for operation with no output load (the ac motor was removed).

The stable operation of the hysteresis controller for the dcoutput voltage is noted. In this test, the hysteresis voltageband was set to 380 V •} 7.5 V. A small part of the figurewas amplified (zoom picture) to analyze the output voltagevariation. It is observed that,when the system reaches 372.5V, at time Th1, the converter starts to operate, and the output voltageincreases at a constant slope. Once it reaches 387.5, at time Th2,the PWM signals are turned off. However, the output voltagestill increases with a different slope between times Th2 andTh3. This is caused by the energy transferred from the inputinductors L1 and L2 through the snubber to the capacitor Cs.Once all the energy is transferred, the PWM signals stay OFFuntil the output voltage decreases reaching again 372.5 V. Atthis voltage level, the system is restarted.Because of the high-frequency nature of the output voltagesupplied to the motor by this converter, it is not trivial to measureits efficiency, at least without very expensive equipment.Considering that, in an induction motor, only the fundamental voltage and current components are converted into mechanicalpower, we based our measurements only in the fundamentaloutput power. A first-order filter was used to obtain the fundamentalcomponent of the voltage, and a digital oscilloscopewas used to obtain the output power of the converter. Fig. 15presents the measured efficiency considering the input powerversus the fundamental power supplied to the motor. A maximumefficiency of 93.64% was obtained for the TIBC firststagedc/dc converter, and that of 91% was obtained for thecomplete system. These curves were obtained during a realoperation with a PV panel, driving the water pump with varyingsolar radiation. The efficiencies take into account all the energyused for the control electronics and drivers and are valid for acommercial prototype.

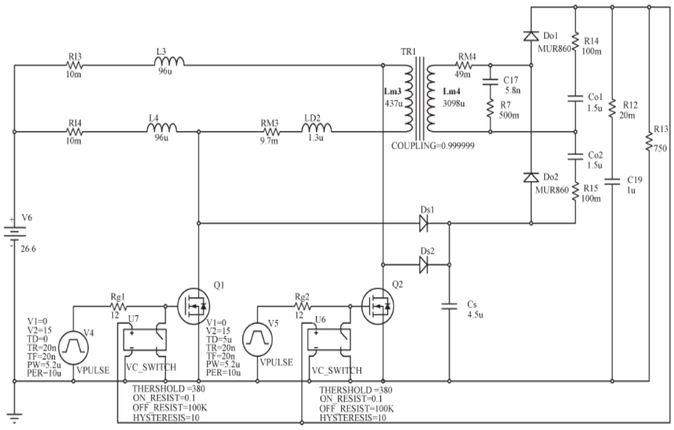

Fig. 7. Circuit used in the simulation.

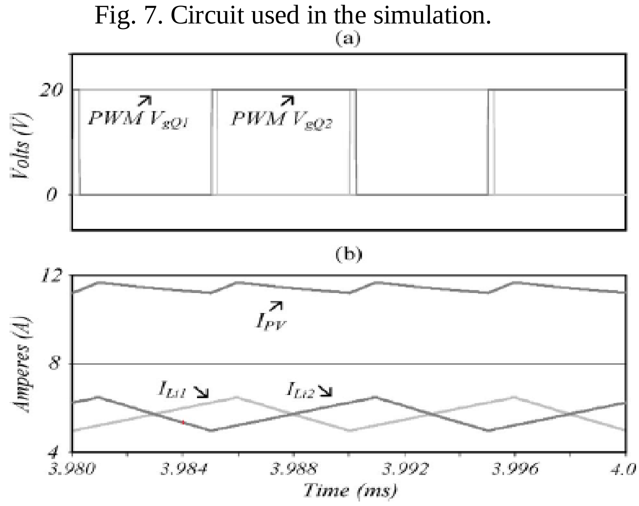

Fig. 8. Simulation results of the input of the dc/dc converter.
(a) Inputswitches' driving signals,
(b) inductors' input currents ILi1 and ILi2, and total input current (IPV).

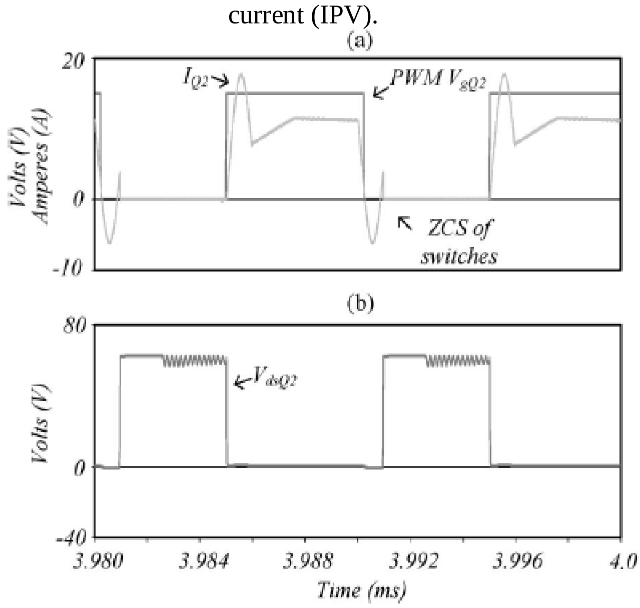

Fig. 9.Verification of the ZCS condition on the input switch *Q*2. (a) *VgQ*2driving signal and *IQ*2 current.
(b) *VdsQ*2 drain–source voltage.

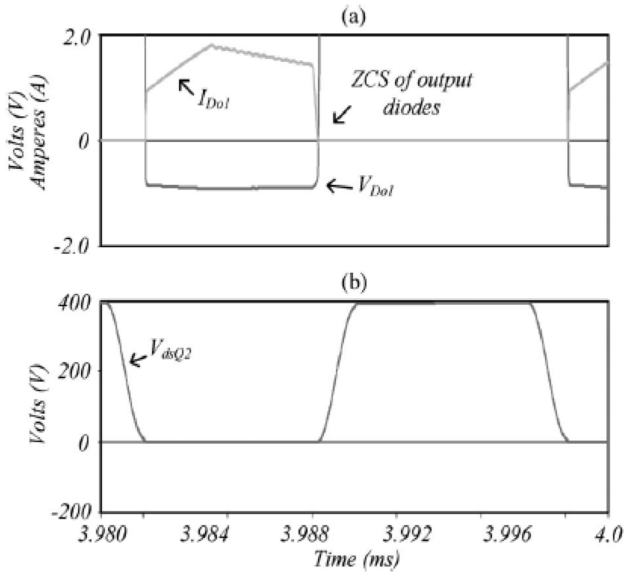

Fig. 10.Verification of the ZCS condition on the rectifying diode *Do*1. (a) Diode *Do*1 current and forward voltage. (b) Diode *Do*1 reverse voltage.

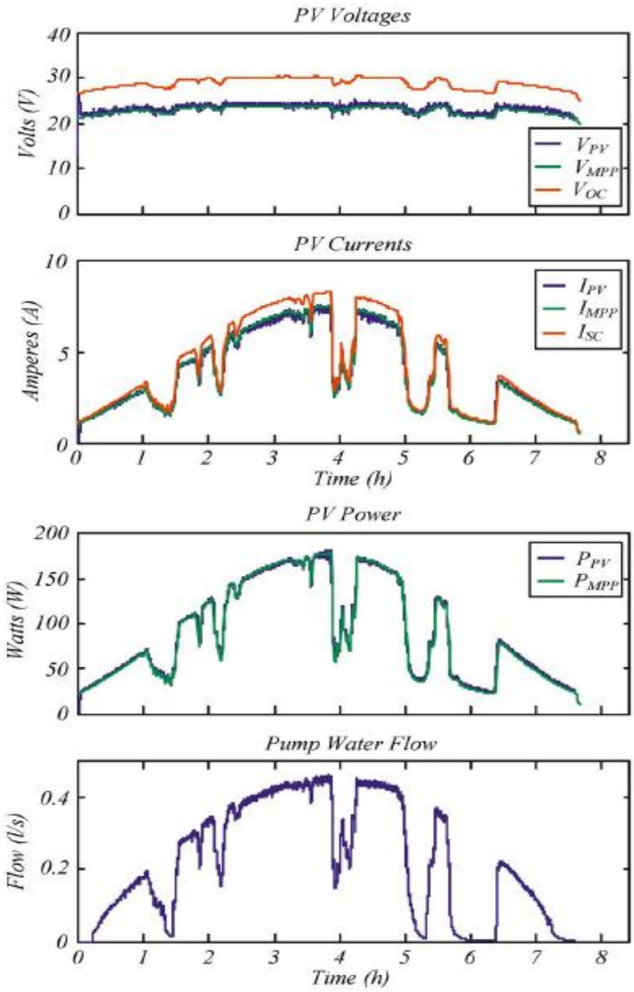

Fig. 11. Voltage and current curves during PV emulation test. Red curvesshow open circuit voltage and short circuit current. Green curves show idealvoltage and current at the MPP. Blue curves show the system voltage andcurrent during the test.

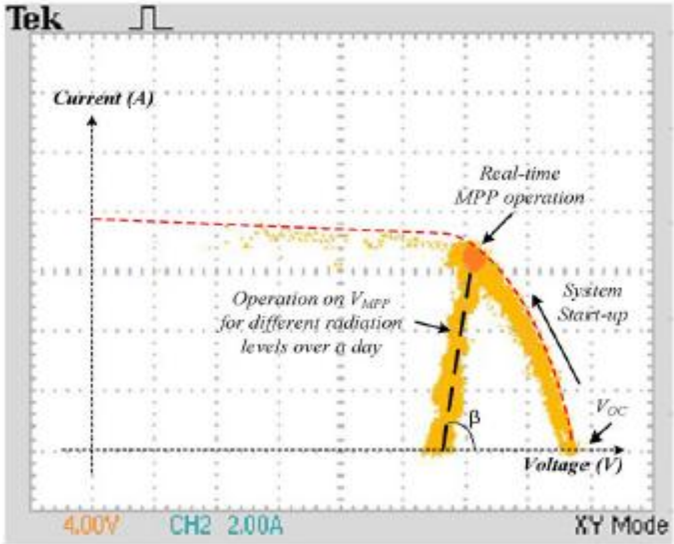

Fig. 12.Real-time MPP operation at a real PV module.

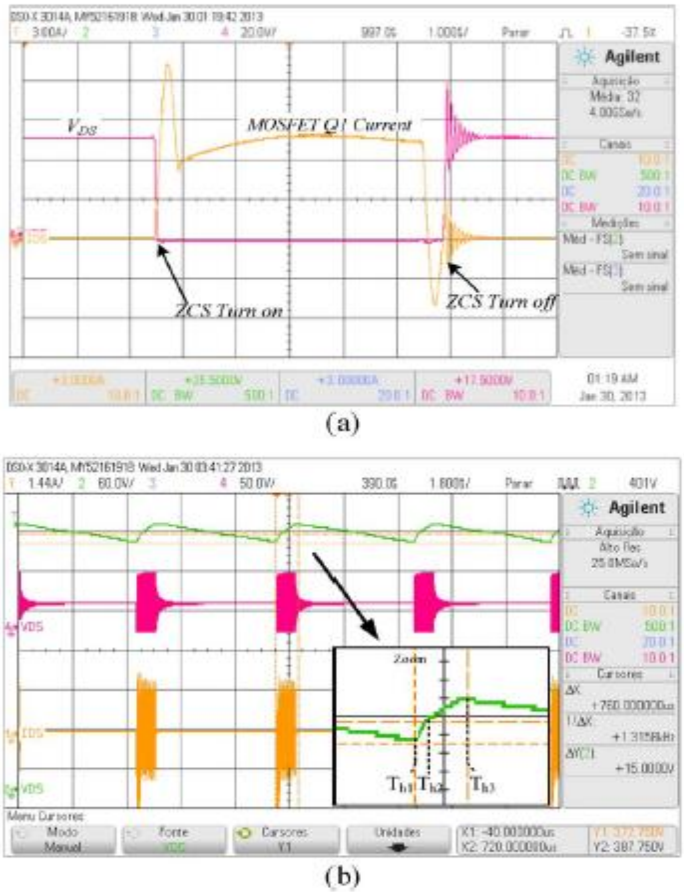

Fig. 13.Voltage and current curves in the MOSFET for two different operationconditions. (a) Drain-to-source voltage and current showing ZCS condition for a MOSFET. (b) Hysteresis control of the output voltage.

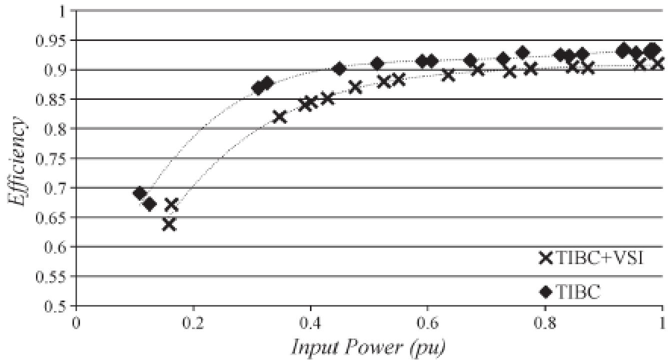

Fig. 14. TIBC and VSI measured efficiency considering only fundamentaloutput power.

VI. CONCLUSION

In this paper, a converter for PV water pumping and treatmentsystems without the use of storage elements was presented.The converter was designed to drive a three-phaseinduction motor directly from PV solar energy and was conceivedto be a commercially viable solution having low cost,high efficiency, and robustness. This paper presented the systemblock diagram, control algorithm, and design. The experimentalresults suggest that the proposed solution could be a viableoption after more reliability tests are performed to guaranteeits robustness.

REFERENCES

[1] M. Chunting, M. B. R. Correa, and J. O. P. Pinto, "The IEEE 2011international future energy challenge—Request for proposals," in *Proc.IFEC*, 2010, pp. 1–24.

[2] A. Hahn, "Technical maturity and reliability of photovoltaic pumping systems,"in *Proc. 13th Eur. Photovoltaic Solar Energy Conf.*, Nice, France,pp. 1783–1786.

[3] M. A. Vitorino and M. B. R. Correa, "High performance photovoltaicpumping system using induction motor," in *Proc. Brazilian Power Electron.Conf.*, 2009, pp. 797–804.

[4] G. Teröde, K. Hameyer, and R. Belmans, "Sensorless control of a permanentmagnet synchronous motor for PV-powered water pump systemsusing the extended Kalman filter," in *Proc. 9th Int. Conf. Elect. Mach.Drives*, 1999, pp. 366–370.

[5] H. Harsono, "Photovoltaic water pump system," Ph.D. dissertation, Dept.Intell. Mech. Syst. Eng., Faculty Kochi Univ. Technol., Kochi, Japan,Aug. 2003.

[6] D. Linden, *Handbook of Batteries and Fuel Cells*. New York, NY, USA:McGraw-Hill, 1984.

[7] D. Tschanz, H. Lovatt, A. Vezzini, and V. Perrenoud, "A multi-functionalconverter for a reduced cost, solar powered, water pump," in *Proc. IEEEISIE*, 2010, pp. 568–572.

[8] M. A. Vitorino, M. B. R. Correa, C. B. Jacobina, and A. M. N. Lima, "Aneffective induction motor control for photovoltaic pumping," *IEEE Trans.Ind. Electron.*, vol. 58, no. 4, pp. 1162–1170, Apr. 2011.

[9] S. R. Bowes and A. Midoun, "Suboptimal switching strategies for microprocessorcontrolled PWM inverter drives," *Proc. Inst. Elect. Eng.—Elect.Power Appl.*, vol. 132, no. 3, pp. 133–148, May 1985.

[10] M. Cacciato, A. Consoli, and V. Crisafulli, "A high voltage gain dc/dc converter for energy harvesting in single module photovoltaic applications,"in *Proc. IEEE ISIE*, 2010, pp. 550–555.

[11] P. J. Wolfs, "A current-sourced dc-dc converter derived via the dualityprinciple from the half-bridge converter," *IEEE Trans. Ind. Electron.*,vol. 40, no. 1, pp. 139–144, Feb. 1993.

[12] P. Wolfs and Q. Li, "An analysis of a resonant half bridge dual converteroperating in continuous and discontinuous modes," in *Proc. IEEE PowerElectron. Spec. Conf.*, 2002, pp. 1313–1318.

[13] W. Li, L. Fan, Y. Zhao, X. He, D. Xu, and B. Wu, "High step-up and highefficiency fuel cell power generation system with active clamp flybackforwardconverter," *IEEE Trans. Ind. Electron.*, vol. 59, no. 1, pp. 599–610, Jan. 2012.

[14] T.-J. Liang, R.-Y.Chen, J.-F.Chen, and W.-J. Tzeng, "Buck-type currentfedpush-pull converter with ZCS for high voltage applications," in *Proc.IEEE Region 10 Conf.*, 2007, pp. 1–4

